

# Creation of Ohmic contact on InGaAs/InAlAs quantum well detector for broad range photon detection

Tamiraa Ganbold<sup>1,\*</sup>, Matias Antonelli<sup>2</sup>, Ralf .H. Menk<sup>2</sup>, Giorgio Biasiol<sup>3</sup>

<sup>1</sup>Department of Chemistry and Biological Engineering, School of Engineering and Applied Science, National University of Mongolia

<sup>2</sup>Elettra – Sincrotrone Trieste S.C.p.A., Trieste, Italy

<sup>3</sup>IOM CNR, Laboratorio TASC, Area Science Park, Trieste, Italy

Several applications utilizing either synchrotron or conventional light sources require fast and efficient pixelated detectors. In order to cover a wide range of experiments, this work investigates the possibility to use InGaAs/InAlAs quantum well devices as photon detectors for a broad range of energies. Owing to their direct, low-energy band gap and high electron mobility, such devices may be used also at room temperature as multi-wavelength sensors from visible light to hard X-rays. Three different metal configurations were tested to create Ohmic contacts on quantum – well detectors. The triple layers of Au/Ge/Ni is a suitable metal to create good Ohmic contacts for the readout electrode. When the beam is hitting from the readout side, Al could be involved as contacting metal with annealing without requiring the etching.

PACS number: 07.85.Qe

Keywords: Ohmic contact, quantum-well photon detector, X-ray .

## INTRODUCTION

As X-ray beams from modern light sources become more intense, with smaller spots and shorter pulse durations, several experimental techniques using either Synchrotron Radiation (SR) or Free Electron Lasers (FEL) would take advantage of new solutions for the production of fast and efficient photon detector [1]. The opportunity to use quantum-well (QW) devices for photon detection has been proposed in infrared region [2]. Thanks to their direct, low-energy band gap and high electron mobility, QW devices based on arsenide semiconductors have been proposed as multi-wavelength sensors from visible light to hard X-rays.

It is very important to create Ohmic contact in both sides of the devices for detector performance such as electronic noise and absorbance of X-ray etc. In order to select the metal for the bias electrode, the photon absorption of the metal layer has to be minimized when the beam is hitting from the bias side. Therefore, the transmission spectra of the all metal configurations were calculated and plotted in terms of incident photon energy (Fig. 1) [3]

In other hand, creating low resistant good contact for readout electrodes is critically important in detector working conditions.

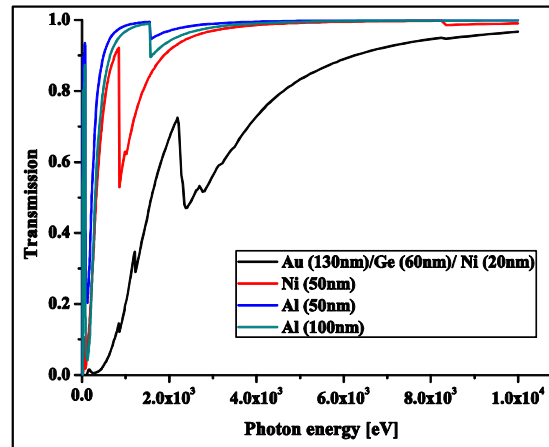


Figure.1. Transmission spectra of all metal layers was calculated.

## DEVICE FABRICATION

InGaAs/InAlAs QWs were grown on a 500- $\mu\text{m}$ -thick, epi-ready semi-insulating GaAs wafer by Molecular Beam Epitaxy (MBE) [3]. In order to virtually eliminate threading dislocations in the QW, a 1- $\mu\text{m}$  step-graded buffer layer (BL) of  $\text{In}_x\text{Al}_{1-x}\text{As}$  ( $x = 0.15 - 0.75$ ) was inserted below the 2DEG region to fit the GaAs lattice parameter to the  $\text{In}_{0.75}\text{Ga}_{0.25}\text{As}$  one (Fig. 2). The BL structure was designed in such a way that its topmost part has a lattice parameter corresponding to the unstrained  $\text{In}_{0.75}\text{Ga}_{0.25}\text{As}$ , owing to the partial lattice relaxation of the buffer layers closer to the substrate. Then, a 25-nm-thick  $\text{In}_{0.75}\text{Ga}_{0.25}\text{As}$  QW containing a 2DEG was placed between 50-nm-thick  $\text{In}_{0.75}\text{Al}_{0.25}\text{As}$

\* Electronic address: tamiraa@seas.num.edu.mn

barrier layers; a delta Si-doping was introduced in the upper barrier at 30 nm distance [4].

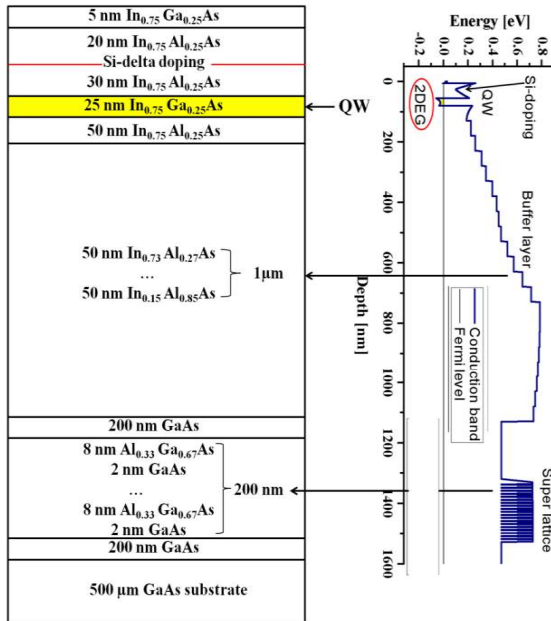


Figure.2. Layered structure of the QW wafer and its band structure showing 2D Electron gas formations.

Due to its low atomic number, Al layer absorbs less the incident photon with respect to the other two metallic layer configurations. Furthermore, it has a less pronounced K absorption edge (1.559 keV). Therefore, a metallic layer of Al can be used as bias electrode when the beam is hitting from the bias side since it has minimum absorption of the photons. Since different pixelation strategies were developed in our devices [5], we have to choose a metal layer creating good Ohmic contact, which can also be useful as a mask for the wet chemical etching for the readout electrode. We developed a test structure to compare the properties of the three metal layers, as is shown in Figure 3. Such structure, repeated for all the three metal configurations (Au/Ge/Ni – 130/60/30nm, Ni-50nm, Al-100nm), consisted of three pads on the surface of the QW side.

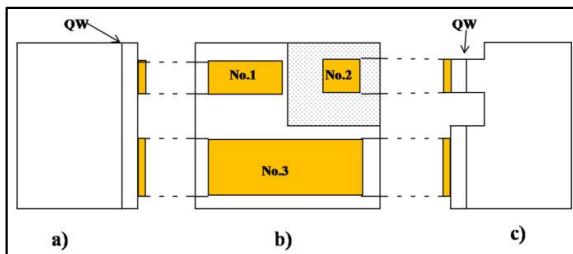


Figure.3. Developed structure to check Ohmic contacts. a) cross section of Pad No.1 and Pad No.3; b) top view of the configuration c) cross section of Pad No.2 and Pad No.3.

Pads No.1 and 3 were deposited on the grown surface and electrically connected through the QW.

Pad No.2 was still deposited on the grown surface, but the QW around the pad was etched away (1.5 μm deep etch), in order to check electrical conduction through the GaAs substrate. Therefore, the resistance  $R_{12}$  measured between Pad No.1 and 2 is of the order of  $M\Omega$  (Fig. 3c) while the resistance  $R_{13}$  between Pad No.1 and 3 of the order of a few  $k\Omega$  (Fig.3a). The metal layers were deposited by a thin film deposition method.

The Au/Ge/Ni metal combination is proven to provide perfectly Ohmic contacts by annealing at 364°C even at cryogenic temperature in InGaAs QW devices [4]. Therefore, Au/Ge/Ni contacts annealed in such a way on our test structure can be considered as the reference of a perfect Ohmic contact.

In other hand, avoiding a double lithographic exposure and the related aligning difficulties, we have used the metal layers themselves as masks to etch the semiconductor. To test the behaviour of the different metals to etching, we performed a blanket etching both through as deposited metal pads and after annealing to 364°C.

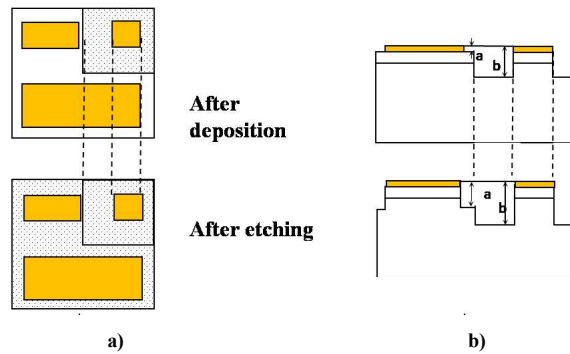


Figure.4. Schematic view of the surface; top view and its cross section; dotted area shows the etched surface.

The samples were etched in the phosphoric etching solution ( $H_3PO_4:H_2O_2:H_2O$  with ratio 3:1:50.) for 15 min with  $\sim 100$  nm/min etching rate after deposition of the metal pads. If the metal layer is capable to withstand the etching solution and protect the underlying semiconductor, the value of  $a$  should be  $\sim 1.5\mu m$ , while  $b$  should be  $\sim 3.0\mu m$  (Fig. 4).

## RESULTS AND DISCUSSION

In order to assess the Ohmic behaviour of the various contacts after deposition then annealing, we have performed I-V scans for  $R_{12}$  in a  $\pm 0.05V$  range (Fig. 5a) and for  $R_{13}$  in a  $\pm 1.0V$  range (Fig. 5b). The curves are all linear, showing a perfect Ohmic character for all the tested contacts, except for Al right after the deposition.  $R_{13}$  resulted of order of  $k\Omega$  for all the metals and becoming a bit lower after the annealing, except for Ni, which increased by an order of magnitude and lost its Ohmic behavior, after the annealing.

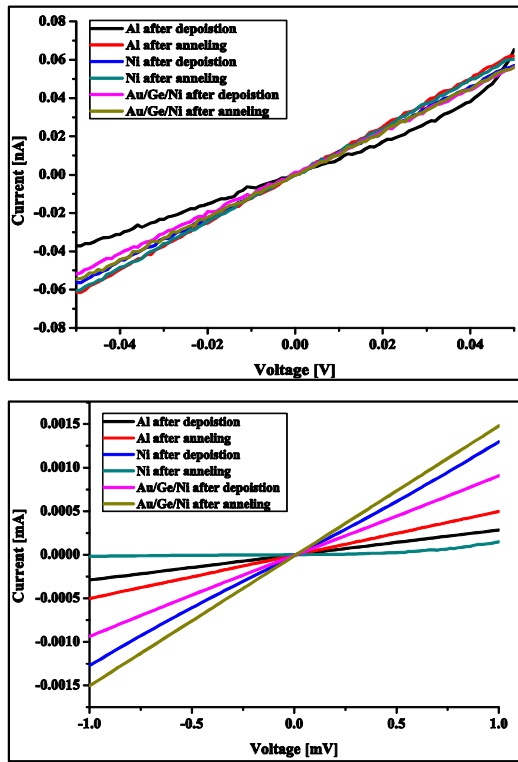


Figure 5. I-V curve for the metals after deposition then annealing.

Table 1. Surface topography of the surface with metal pads before and after etching.

	Au/Ge/Ni	Al	Ni
Etched after deposition	a=2.1μm b=3.6μm	a=0.4μm b=2.0μm	a=1.9μm b=3.3μm
Etched after annealing	a=1.6μm b=3.3μm	a=2.0μm b=3.3μm	a=0.6μm b=1.2μm

As shown in Table 1, the Au/Ge/Ni triple layer was not attached by the solution even after annealing and etching. However, Ni could resist the chemical etching only when it is not annealed and Al only after annealing. Annealed Ni and just deposited Al layers were etched and the QW surface as well. The ability of the different metals to sustain etching must be however confirmed by measuring the resistances between the pads (Fig. 6).

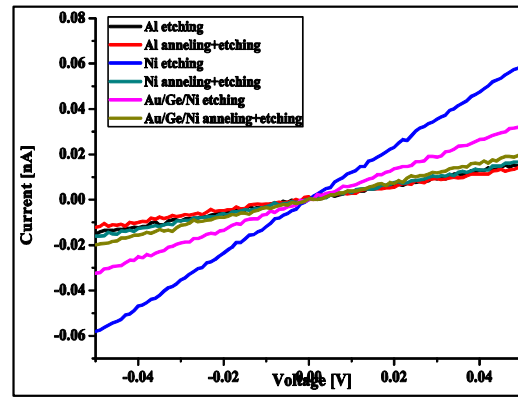
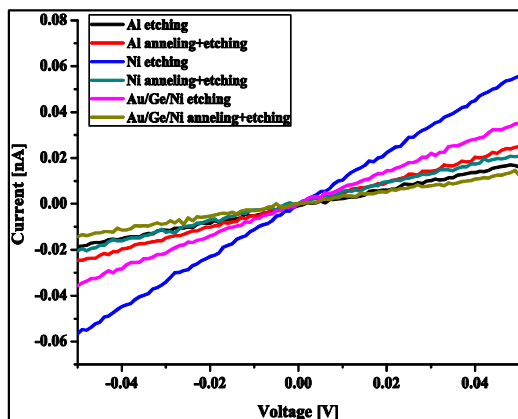


Figure 6. I-V curve for the metals etching after deposition, etching and annealing.

The resistance  $R_{12}$  between Pad No.1 and 2 of Au/Ge/Ni and Ni before and after etching the as deposited metals was similar, while it increased considerably for Al, implying that Al was etched away by the solution. The resistances  $R_{13}$  between Pad No.1 and 3 after etching in the phosphoric solution increased to the order of the substrate resistance. However, Au/Ge/Ni and Ni metal layers are still resulting same order of  $R_{12}$  even after annealing and etching.

Table 2. Summarizing  $R_{12}$  and  $R_{13}$  for all the cases with three tested metals.

Procedure	Au/Ge/Ni		Ni		Al	
	$R_{12}$	$R_{13}$	$R_{12}$	$R_{13}$	$R_{12}$	$R_{13}$
After deposition	93 MΩ	2.2 kΩ	87 MΩ	1.6 kΩ	113 MΩ	6.9 kΩ
After annealing	89 MΩ	1.3 kΩ	81 MΩ	35 kΩ	80 MΩ	4.0 kΩ
After etching	153 MΩ	142 MΩ	84 MΩ	88 MΩ	327 MΩ	277 MΩ
After annealing then etching	253 MΩ	364 MΩ	303 MΩ	239 MΩ	380 MΩ	201 MΩ

### CONCLUSIONS

As a conclusion, a triple layers of Au/Ge/Ni is a suitable metal to create good Ohmic contacts for the readout electrode. Moreover, Au/Ge/Ni and Ni metal layers could be used as a protecting mask due to the capability to resist the etching solution. However, the metallic layer should not be annealed before the etching and it can be annealed later. When the beam is hitting from the readout side, Al could be involved as contacting metal with annealing without requiring the etching.

**ACKNOWLEDGEMENTS**

We acknowledges support from the Training and Research in Italian Laboratories (TRIL) Programme of the International Centre for Theoretical Physics, Trieste. The research leading to these results has received funding from the European Community's Seventh Framework Programme (FP7/2007-2013) under grant agreement no 312284.

**REFERENCES**

- [1] R. G. VanSilfhout, S. Manolopoulos, N. R. Kyele, and K. Decanniere, *Sens. Actuat. A* 133, 82 (2007).
- [2] J. K. L. S. V. Bandara, S. D. Gunapala, D. Z-Y. Ting, S. B. Rafol, *Proc.Far-IR, Sub-Mm MM Detect. Technol. Work.* (2002).
- [3] B. L. Henke, E. M. Gullikson, and J. C. Davis, *At. Data Nucl. Data Tables* 54, 181 (1993).
- [4] F. Capotondi, G. Biasiol, D. Ercolani, V. Grillo, E. Carlino, F. Romanato, and L. Sorba, *Thin Solid Films* 484, 400 (2005).
- [5] F. Capotondi, G. Biasiol, I. Vobornik, L. Sorba, F. Giazotto, A. Cavallini, and B. Fraboni, *J. Vac. Sci. Technol. B* 22, 702 (2004).
- [6] T. Ganbold, M. Antonelli, G. Biasiol, G. Cautero, H. Jark, D. M. Eichert, R. Cucini, and R. H. Menk, *J. Instrum* 9, (2014).